

Measurements of hardness, young's modulus, and fracture toughness of solar grade silicon obtained from metallurgical grade silicon

Denir Paganini Nascimento^{1*} 

Marcelo Aquino Martorano¹ 

Caio Cesar Cebalos de Almeida¹ 

Angelo Fernando Padilha¹ 

Abstract

Young modulus and toughness (K_{IC}) of bulk solar grade silicon (SoG-Si) obtained by directional solidification of metallurgical grade silicon were determined. The Young modulus was measured by the technique of impulse excitation of vibration and K_{IC} was determined using the indentation method. Measurement values agree well with those available in the literature. The indentation method proved to be a reliable, relatively simple, inexpensive, and fast experimental method to measure K_{IC} in SoG-Si.

Keywords: Solar grade silicon; Young's modulus; Toughness; Indentation method.

1 Introduction

Silicon is one of the most frequent chemical elements in the earth crust and is broadly used in a wide variety of applications ranging from traditional metallurgy to microelectronic devices and photovoltaic cells. The demand for solar grade silicon (SoG-Si) has been growing rapidly in the past decades and new, more economic production routes have been researched. An interesting alternative route to obtain SoG-Si is the metallurgical route, which consists of refining metallurgical grade silicon (MG-Si), containing about 98.5% Si, to attain the purity of the SoG-Si. An important process step in this route is the directional solidification of the MG-Si [1-5] to induce segregation of metallic impurities to the silicon ingot top. Although mechanical properties of silicon play a secondary role in the efficiency of photovoltaic cells [6], its lack of ductility [7] and toughness [8] affects the production of silicon wafers and solar panels and makes the mechanical conformation of silicon practically impossible. Toughness measurements of SoG-Si produced by directional solidification of MG-Si are not easily found in the literature.

Since silicon is very brittle, its K_{IC} could be easily measured by the indentation method [9,10], which is a fast, low-cost, and convenient method. The aim of the present work is to measure the K_{IC} by the indentation method of a solar grade silicon (SoG-Si) obtained by the directional solidification of a metallurgical grade silicon (MG-Si). To use this method, the Young's modulus of the SoG-Si must be known with sufficient accuracy. Therefore, the Young's

modulus of the SoG-Si was also determined in the present work by the technique of impulse excitation of vibration [11].

2 Experimental procedures

2.1 Casting of silicon ingots

Two samples were extracted from two different ingots of polycrystalline silicon, one of MG-Si and another of SoG-Si obtained from the melting and subsequent directional solidification of the MG-Si. The scheme of the directional solidification furnace is shown in Figure 1. It consists of two chambers. In one of the chambers, at the bottom, there is a water-cooled copper base for heat extraction. At the top of the furnace, in the upper chamber, there are heating elements of $MoSi_2$ to increase the thermal gradient applied to the solidification front. A disc, connected to an electrical motor through a shaft, rotated within the melt to enhance liquid homogenization and increase segregation of impurities to the ingot top. The lateral wall of the crucible containing the melt is thermally insulated by refractory blocks to promote directional solidification.

Concentrations of the main metallic impurities were determined for the two ingots by Inductively Coupled Plasma-Optic Emission Spectrometry (ICP-OES). The composition of the MG-Si ingots was (in ppmw): Fe (1368); Al (290); Zr (75); Ti (69); Mn (51); Cu (9) and Ni (6). In the SoG-Si

¹Departamento de Engenharia Metalúrgica e de Materiais, Universidade de São Paulo, USP, São Paulo, SP, Brasil.

*Corresponding author: dpnascimento@usp.br.



ingot, however, only Al (less than 4 ppm) and Ni (less than 2 ppm) were detected, whereas the concentrations of the remaining elements were below the quantification limit of the analytical procedures.

2.2 Young's modulus measurements

The Young's modulus was measured by the method of impulse excitation of vibration using two modes flexural + torsional and flexural [11] in rectangular section specimens of dimensions 10 x 14 x 45 mm. The specimens were cut off from the ingot with a diamond wire sawing machine, which provides precise cuts with minimal material loss, minimal pressure, and practically without heat generation during the cutting process.

2.3 Vickers hardness measurements

The Vickers hardness was determined (GPa) using the following Equation 1 [12]

$$H_v = \frac{18544L}{d^2} \quad (1)$$

Where L is the applied load (kgf) and d is the length (μm) of the diagonal of the indentation.

2.4 K_{IC} measurements

Toughness (K_{IC}) was calculated ($\text{MPa}\cdot\text{m}^{1/2}$) as follows [13]

$$K_{IC} = 0.035 \left(\frac{l}{a} \right)^{\frac{1}{2}} \left(\frac{E \cdot \beta}{H_v} \right)^{0.4} \frac{H_v \sqrt{a}}{\beta} \quad (2)$$

Where l is the crack length, a is the length of indentation half-diagonal, and $\beta = 3$ is the constraint factor. Cracks formed on the polished surface of the silicon ingot samples during the Vickers indentation procedure. Crack formation is a necessary condition to determine the K_{IC} by the indentation method using Equation 2. After several preliminary tests to select a load (L) that causes the formation of cracks around indentation marks in both SoG-Si and MG-Si samples, 100 gf was chosen.

2.5 Microstructural analysis

Complementary techniques of microstructural analysis, such as X-ray diffraction and scanning electron microscopy (SEM) with energy-dispersive X-ray spectrometry (SEM/EDS) microanalysis were used to characterize the microstructure of the samples.

3 Results and discussion

The columnar grain structure of the polycrystalline SoG-Si and MG-Si ingots from which the samples were

extracted are shown in Figure 2 and 3, respectively. The samples contained several grains and the arrows indicate the locations where they were extracted from. The Young's modulus of the SoG-Si determined from 10 measurements was 89.51 ± 0.05 GPa using the torsional/flexural vibration mode and 89.45 ± 0.13 GPa using the flexural mode. Figure 4 shows micrographs from observations in the scanning electron microscope (SEM) of the SoG-Si sample with secondary electrons (Figure 4a) and backscattered electrons (Figure 4b). The Vickers hardness, determined from 20 measurements, was 10.40 ± 0.35 GPa, while the K_{IC} value obtained from Equation 2 after measuring the lengths of the cracks was 0.81 ± 0.04 $\text{MPa}\cdot\text{m}^{1/2}$.

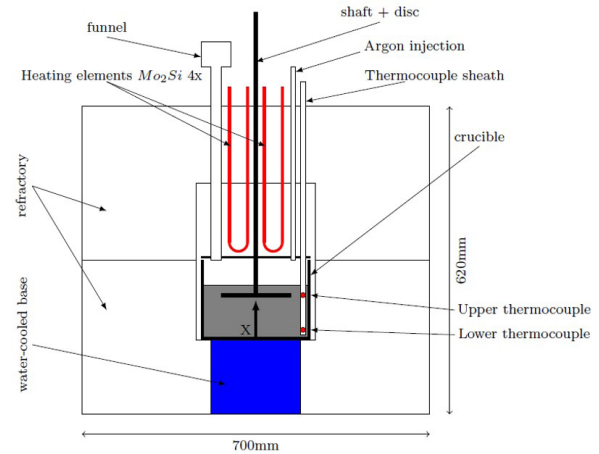


Figure 1. Schematic drawing of the directional solidification furnace used to obtain SoG-Si.

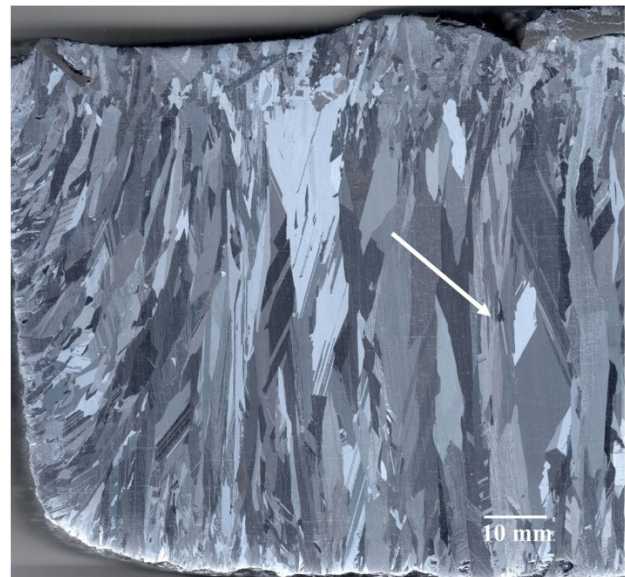


Figure 2. Columnar grain structure of the longitudinal section of the SoG-Si cylindrical ingot obtained by directional solidification. The arrow indicates the location from where the sample was extracted. Etchant: NaOH 20% at 90 °C for 20 minutes.

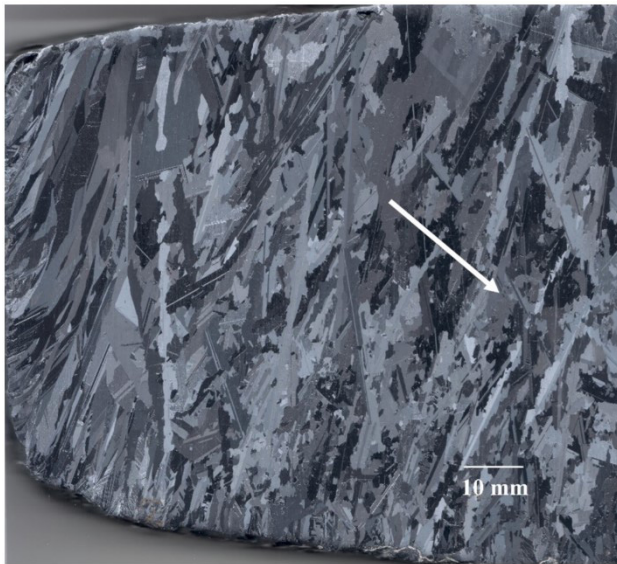


Figure 3. Columnar grain structure of the longitudinal section of the MG-Si cylindrical ingot obtained by directional solidification. The arrow indicates the location from where the sample was extracted. Etchant: NaOH 20% at 90 °C for 20 minutes.

Figure 5 shows SEM micrographs of the MG-Si using secondary electrons. The hardness marks on the MG-Si were more irregular and flakes were detached in some indentations occasionally, as shown in Figure 5a. Nevertheless, measurements were carried out when flakes were absent, as shown in Figure 5b. Owing to its purity level, the SoG-Si was free from intermetallic particles, but particles containing Al, Fe, Mn, Ti, and Si were found in the MG-Si (Figure 6). Microanalyses by energy-dispersive X-ray spectroscopy (EDS) were carried out in several particles. One of the particles is given in Figure 7 and the corresponding energy spectrum obtained with the EDS analysis is given in Figure 8, showing results similar to those reported by Vogelaar [14].

The Vickers hardness in the MG-Si was 10.50 ± 0.45 GPa. Determination of the Young's modulus in the MG-Si sample was not possible owing to limitations of the sample size. However, the Young's modulus measured for the SoG-Si was used in Equation 2 to calculate the K_{IC} for the MG-Si from Equation 2, resulting in 0.84 ± 0.05 MPa.m^{1/2}.

The hardness measurement values obtained in the present work compare reasonably well with those available

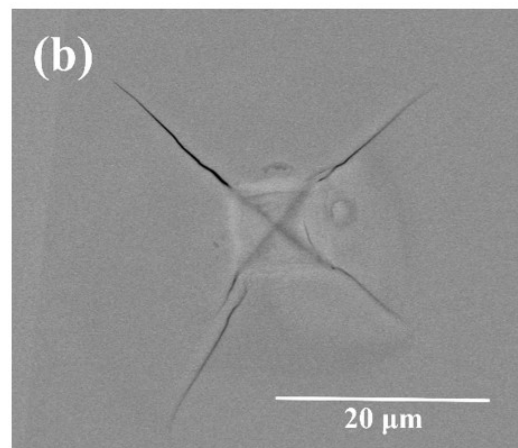
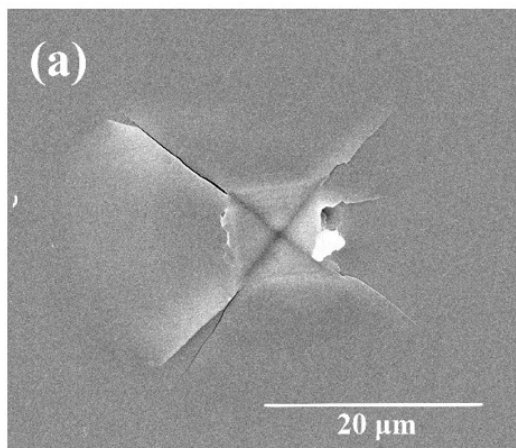


Figure 4. Vickers indentations (load of 100 gf) in SoG-Si observed with scanning electron microscope using contrast of: a) secondary electrons and b) backscattered electrons.

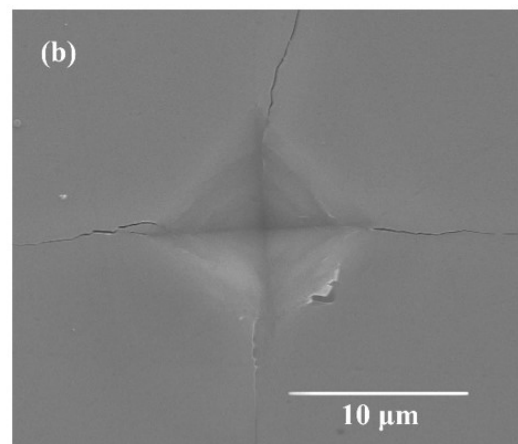
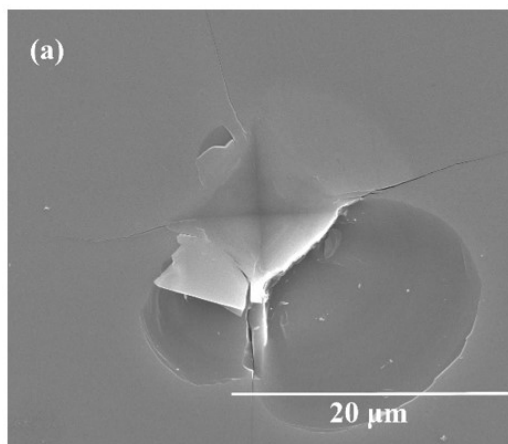


Figure 5. Vickers indentations (load of 100 gf) in MG-Si observed with scanning electron microscope using secondary electrons.

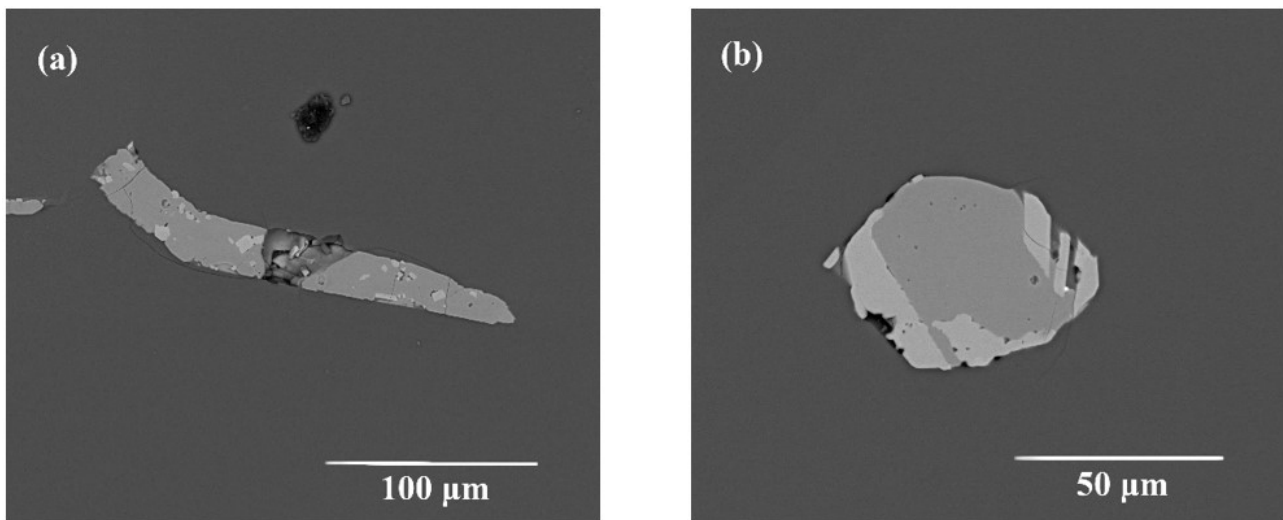


Figure 6. Intermetallic particles observed with backscattered electrons (SEM) in MG-Si.

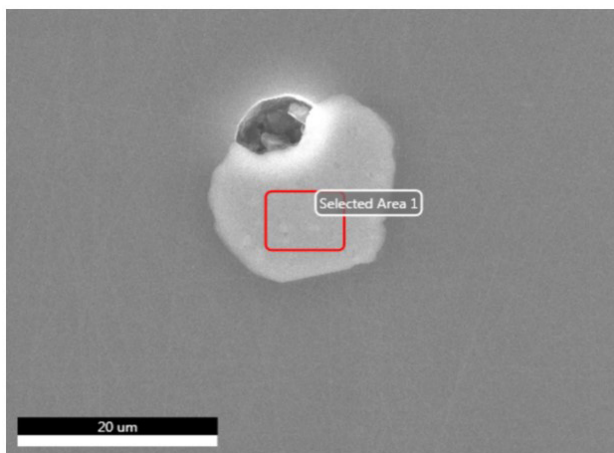


Figure 7. Intermetallic particle observed with backscattered electrons (SEM) in MG-Si, where microanalyses with energy-dispersive X-ray spectroscopy (EDS) were carried out.

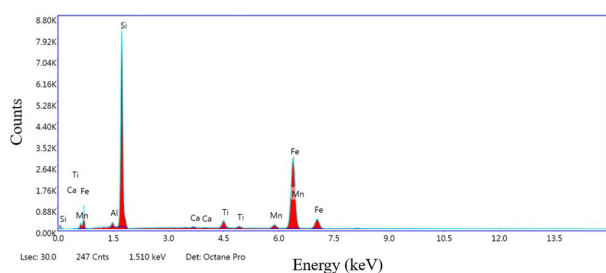


Figure 8. Energy spectrum obtained with the energy-dispersive X-ray spectroscopy (EDS) of the selected area of the particle in Figure 7.

in the literature. For example, Schilz and Langenbach [15] found 12.40 GPa (HV1) for bulk fine-grained silicon obtained by hot-isostatic pressing. With respect to K_{IC} , Brodie and Bahr [8] found approximately $1.7 \text{ MPa}\cdot\text{m}^{1/2}$ for fine-grained silicon. Although the measurement of K_{IC} by the indentation

method is relatively easy, the steps described next should be carried out carefully. The load should be selected to cause cracks around the indentation mark, as the length of cracks is required in Equation 2. There are several formulas available in the literature to calculate K_{IC} [10], but Equation 2 was chosen because it is one of the most used [10]. The Young's modulus of the material should be known with reasonable accuracy, specially if its elastic properties are highly anisotropic, as is the case of silicon [16,17].

4 Conclusions

The main conclusions of this work are:

- 1) The metallurgical processing route used to purify the metallurgical grade silicon (MG-Si) allows obtaining cylindrical polycrystalline ingots of solar grade silicon (SoG-Si) with adequate purity.
- 2) The combination of relatively simple characterization techniques allows a rapid assessment of the hardness, Young's modulus, and toughness of silicon.
- 3) The solar grade silicon (SoG-Si) and metallurgical grade silicon (MG-Si), although having significantly different levels of purity, exhibit almost identical hardness and toughness.

Acknowledgements

Authors thank the support from Fundação de Amparo à Pesquisa do Estado de São Paulo, FAPESP (2017/22361-6). We also thank Prof. Dr. Katia Cristine Gandolpho Candioto (EEL-USP) and the PhD student Emanuelle Machado Amaral (PMT-USP) for their help in the Young's modulus measurements.

References

- 1 Lima ML, Martorano MA, Ferreira JB No. Macrosegregation of impurities in a metallurgical silicon ingot after transient directional solidification. *Materials Research*. 2017 [cited 2022 June 16];20(4):1129-1135. Available at: http://www.scielo.br/scielo.php?script=sci_arttext&pid=S1516-14392017000401129&lng=en&tlng=en
- 2 Lei Y, Ma X, Wang Y, Chen Z, Ren Y, Ma W, et al. Recent progress in upgrading metallurgical-grade silicon to solar-grade silicon via pyrometallurgical routes. *International Journal of Minerals, Metallurgy and Materials*. 2022 [cited 2022 June 16];29(4):767-782. Available at: <https://link.springer.com/article/10.1007/s12613-022-2418-3>
3. Martorano MA, Ferreira Neto JB, Oliveira TS, Tsubaki TO. Refining of metallurgical silicon by directional solidification. *Materials Science and Engineering: B*. 2011;176(3):217-226. <http://dx.doi.org/10.1016/j.mseb.2010.11.010>
- 4 Chigondo F. From metallurgical-grade to solar-grade silicon: an overview. *Silicon*. 2018 [cited 2022 June 16];10(3):789-798. Available at: <https://link.springer.com/article/10.1007/s12633-016-9532-7>
- 5 Marques FC, Cortes ADS, Mei PR. Solar cells fabricated in upgraded metallurgical silicon, obtained through vacuum degassing and czochralski growth. *Silicon*. 2019 [cited 2022 June 16];11(1):77-83. Available at: <http://link.springer.com/10.1007/s12633-018-9860-x>
- 6 Louwen A, van Sark W, Schropp R, Faaij A. A cost roadmap for silicon heterojunction solar cells. *Solar Energy Materials and Solar Cells*. 2016 [cited 2022 June 16];147:295-314. Available at: <https://linkinghub.elsevier.com/retrieve/pii/S0927024815006741>
- 7 Wu M, Murphy JD, Jiang J, Wilshaw PR, Wilkinson AJ. Microstructural evolution of mechanically deformed polycrystalline silicon for kerfless photovoltaics. *Physica Status Solidi*. 2019 [cited 2022 June 16];216(10):1800578. Available at: <https://onlinelibrary.wiley.com/doi/full/10.1002/pssa.201800578>
- 8 Brodie R, Bahr D. Fracture of polycrystalline silicon. *Materials Science and Engineering: A*. 2003 [cited 2022 June 16];351(1–2):166-173. Available at: <https://linkinghub.elsevier.com/retrieve/pii/S0921509302008298>
- 9 Anstis GR, Chantikul P, Lawn BR, Marshall DB. A critical evaluation of indentation techniques for measuring fracture toughness: I, direct crack measurements. *Journal of the American Ceramic Society*. 1981 [cited 2022 June 16];64(9):533-538. Available at: <https://onlinelibrary.wiley.com/doi/full/10.1111/j.1151-2916.1981.tb10320.x>
- 10 Şakar-Deliormanli A, Güden M. Microhardness and fracture toughness of dental materials by indentation method. *Journal of Biomedical Materials Research. Part B, Applied Biomaterials*. 2006 [cited 2022 June 16];76B(2):257-264. Available at: <https://onlinelibrary.wiley.com/doi/full/10.1002/jbm.b.30371>
- 11 ASTM International [Internet]. Standard test method for dynamic young's modulus, shear modulus, and poisson's ratio by impulse excitation of vibration [cited 2022 June 16]. Available at: <https://www.astm.org/e1876-21.html?mscclkid=bd3bea7bd14411ecb7f2db394c27f698>
- 12 ASTM International [Internet]. Standard test methods for vickers hardness and knoop hardness of metallic materials [cited 2022 June 16]. Available at: <https://www.astm.org/standards/e92?mscclkid=14608947d14511ecb54e967ca80fc100>
- 13 Bowen P, Bonjour C, Carry C, Gonseth D, Hofmann H, Mari D, et al. Novel alumina titanium-carbonitride nickel composites. *JOM*. 1995 [cited 2022 June 16];47(11):56-58. Available at: <http://link.springer.com/10.1007/BF03221312>
- 14 Vogelaar GC. Analysis of intermetallic phases in silicon ingots of different thickness. In: Oye HA, Rong HM, Ceccaroli B, Nygaard L, Tuset JK, editors. *Silicon for the chemical and solar industry III*. Sandefjord: The Norwegian University of Science and Technology (NTNU); 1996. p. 95-112.
- 15 Schilz J, Langenbach M. Powder metallurgy of Ge, Si, and Ge-Si. *Journal of Crystal Growth*. 1993 [cited 2022 June 16];128(1–4):1197-1202. Available at: <https://linkinghub.elsevier.com/retrieve/pii/S0022024807801230>
- 16 Hopcroft MA, Nix WD, Kenny TW. What is the young's modulus of silicon? *Journal of Microelectromechanical Systems*. 2010 [cited 2022 June 16];19(2):229-238. Available at: <http://ieeexplore.ieee.org/document/5430873/>
- 17 Paggi M, Corrado M, Reinoso J. Fracture of solar-grade anisotropic polycrystalline Silicon: a combined phase field-cohesive zone model approach. *Computer Methods in Applied Mechanics and Engineering*. 2018 [cited 2022 June 16];330:123-148. Available at: <https://www.sciencedirect.com/science/article/pii/S0045782517306928>

Received: 16 June 2022

Accepted: 17 Nov. 2022